

Prediction and Evaluation of Protein Farnesyltransferase Inhibition by Commercial Drugs

Amanda J. DeGraw,[†] Michael J. Keiser,[‡] Joshua D. Ochocki,[†] Brian K. Shoichet,^{*,‡} and Mark D. Distefano^{*,†}

[†]Department of Chemistry, University of Minnesota, 207 Pleasant Street SE, Minneapolis, Minnesota 55455, and [‡]Department of Pharmaceutical Chemistry, University of California San Francisco, 1700 4th Street, San Francisco, California 94158

Received November 3, 2009

The similarity ensemble approach (SEA) relates proteins based on the set-wise chemical similarity among their ligands. It can be used to rapidly search large compound databases and to build cross-target similarity maps. The emerging maps relate targets in ways that reveal relationships one might not recognize based on sequence or structural similarities alone. SEA has previously revealed cross talk between drugs acting primarily on G-protein coupled receptors (GPCRs). Here we used SEA to look for potential off-target inhibition of the enzyme protein farnesyltransferase (PFTase) by commercially available drugs. The inhibition of PFTase has profound consequences for oncogenesis, as well as a number of other diseases. In the present study, two commercial drugs, Loratadine and Miconazole, were identified as potential ligands for PFTase and subsequently confirmed as such experimentally. These results point toward the applicability of SEA for the prediction of not only GPCR–GPCR drug cross talk but also GPCR–enzyme and enzyme–enzyme drug cross talk.

Introduction

Bringing a novel chemical entity to market cost 868 million USD in 2006,¹ with most costs accumulating during clinical testing when drug candidates fail due to unforeseen pathway interactions. While these interactions are often harmful, causing adverse effects, they may also be beneficial, leading to useful properties. Accurate prediction of off-target drug activity prior to clinical testing may benefit patient safety and also lead to new therapeutic indications, as has been promoted by Wermuth, among others.^{2–5}

The similarity ensemble approach (SEA^a) uses chemical similarity among ligands organized by their targets to calculate similarities among those targets and to predict drug off-target activity.^{6–8} From the perspective of molecular pharmacology and bioinformatics, the approach is counter-intuitive, as it relies on ligand chemical information exclusively, using no target structure or sequence information whatsoever. Instead, SEA and related cheminformatics approaches^{9–15} return to an older, classical pharmacology view, where biological targets were characterized by the ligands that bind to them. To that older view, SEA adds modern methods for measuring chemical similarity for sets of ligands and applies the BLAST¹⁶ sequence-similarity algorithms to control for the similarity among ligands and ligand sets that one would expect at random (an innovation of this method).^{7,17} The technique has been used to discover several drugs activities at unanticipated targets. The opioid receptor antagonists

methadone and loperamide were predicted and subsequently found to be ligands of the muscarinic and neurokinin NK2 receptors, respectively.⁷ More recently, the antihistamines dimetholizine and mebhydrolin base were predicted and found to have activities against α_1 adrenergic, 5-HT_{1A} and D₄ receptors, and 5-HT_{5A}, respectively, the anticholinergic diphenamil methylsulfate was predicted and found to have δ -opioid activity, the transport inhibitor fluoxetine was predicted and found to bind to the β_1 -adrenergic receptor, and the α_1 blocker indoramin was predicted and found to have dopamine D₄ activity, among others.^{6–8}

Many of these predictions have been among drugs that bind aminergic G-protein coupled receptors (GPCRs),^{6–8} and whereas there have been cases of predictions crossing receptor classification boundaries (e.g., ion channel blockers acting on GPCRs and transporters⁸), a criticism to which the approach may be liable is that it has been focused on targets for which polypharmacology is not without precedent. We thought it interesting to investigate whether off-target activity may be predicted for drugs that target enzymes, especially for those drugs predicted to be active against an enzyme that has little or no similarity to the canonical target for that drug. As a target enzyme we focused on protein farnesyltransferase (PFTase), using SEA to compare 746 commercial drugs against ligand sets built from the 1640 known nonpeptide PFTase ligands reported in ligand–receptor annotation databases (see General Materials and Methods).

The post-translational attachment of lipid moieties to proteins is critical for membrane anchorage of signal transduction proteins.¹⁸ PFTase catalyzes the attachment of the C₁₅ isoprenoid to a cysteine residue of proteins containing a C-terminal CAAX consensus sequence, where C is the cysteine to be prenylated, A is an aliphatic amino acid, and X is commonly Ser or Met.¹⁹ Upon attachment of the isoprene unit, an endoprotease cleaves off the –AAX residues. Using *S*-adenosylmethionine as a methyl-group donor, a

*To whom correspondence can be addressed: For M.D.D.: phone, 612-624-0544; fax, 612-626-7541; E-mail: diste001@umn.edu. For B.K.S.: phone, 415-514-4126; fax, 415-502-1411; E-mail, shoichet@cgl.ucsf.edu.

^aAbbreviations: SEA, similarity ensemble approach; GPCRs, G-protein coupled receptors; PFTase, protein farnesyltransferase; FTIs, farnesyltransferase inhibitors; TPIT, tetraiodophenolphthalein; GFP, green fluorescent protein; WOMBAT, World of Molecular BioActivity.

Table 1. Top SEA Predictions of Off-Target PFTase Binding for Commercial Drugs^a

	Drug	Best SEA E-value	Best FTI Match
1	Loratadine	1.07×10^{-81}	10 μM
2	Rupatadine	1.10×10^{-49}	10 μM
3	Desloratadine	1.22×10^{-30}	10 μM
4	Ubenimex	1.53×10^{-16}	100 μM
5	Azatadine	2.68×10^{-11}	100 μM
6	Phenylalanine S	1.70×10^{-4}	100 μM
7	Miconazole	2.00×10^{-4}	100 μM
8	Diazepam ⁷⁰	5.52×10^{-4}	1 μM
9	Temazepam ⁷⁰	1.21×10^{-3}	1 μM
10	Thymopentin	2.10×10^{-3}	100 μM
11	Cortisone acetate ⁶³	6.57×10^{-3}	100 μM
12	Prednisone ⁶³	3.81×10^{-2}	100 μM

^a Drugs in red have PFTase activity already reported in the literature. Drugs in blue were either peptides or unavailable.

methyltransferase then caps the $-\text{COOH}$ of the prenylated protein. It is the increase in hydrophobicity, as well as the lack of charge at the C-terminus, that allows for membrane localization.²⁰ Proteins that are farnesylated include the nuclear lamins and members of the Ras superfamily of small guanosine triphosphatases.²⁰

The finding that mutant Ras proteins must be prenylated to exert their oncogenic effects^{21,22} lead to the development of a number of inhibitors of protein prenylation, specifically through the inhibition of PFTase. Compounds were either rationally designed, based on peptide- or isoprenoid-substrate characteristics, or were discovered through screening of in-house chemical libraries. To date, five compounds have been brought to clinical trials as inhibitors of PFTase.²³ Results of these trials have been modest at best, with very few compounds showing antitumor activity.^{23–25} Two drug candidates, Lonafarnib (Schering-Plough) and Tipifarnib (Janssen Pharmaceutica), are the only compounds to make it to late-stage clinical trials²⁶ and are currently being explored as single agents or adjunct therapies for breast cancer²⁷ and leukemia.^{28,29}

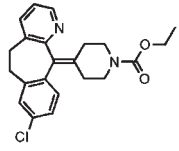
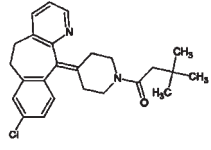
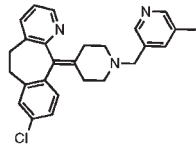
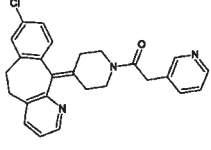
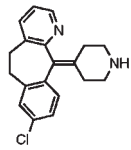
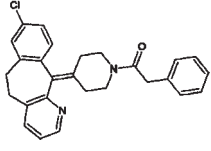
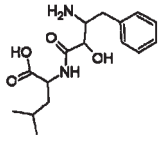
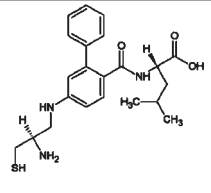
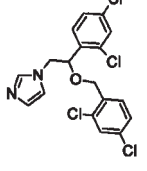
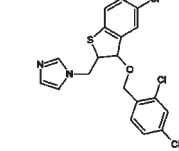
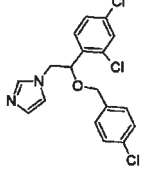
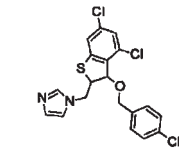
While farnesyltransferase inhibitors (FTIs) have yet to live up to their promise as anticancer agents, they are showing applicability toward the treatment of other diseases. Hutchinson–Gilford Progeria syndrome results from a mutation in the LMNA gene, which causes an unusable form of the protein Lamin A. Because the precursor to Lamin A is farnesylated, it was proposed that FTIs may be capable of ameliorating the disease phenotypes in those suffering from progeria.³⁰ Studies published in 2006 found that treatment of progeria mice with the FTI Lonafarnib could dramatically prevent the development of disease characteristics.^{31,32} These results prompted the launch of a phase II clinical trial examining the use of Lonafarnib in progeria patients.³³ FTIs are also capable of blocking farnesylation in the protozoan parasites *Trypanosoma cruzi*, *Trypanosoma brucei*, and *Plasmodium falciparum*.³⁴ The cessation of farnesylation in these parasites by inhibiting PFTase appears to be particularly toxic, indicating the potential of FTIs for the treatment of Chagas disease³⁵ (caused by *T. cruzi*), African sleeping sickness³⁶

(caused by *T. brucei*), and malaria^{37,38} (caused by *P. falciparum*). The clinical relevance of FTIs toward a number of diseases necessitates the development of more potent and selective inhibitors. A starting point for identifying new PFTase inhibitors is exploring those drugs already in use for other diseases.

Results

Applying SEA to Protein Farnesyltransferase. To predict which compounds may have off-target activity against PFTase, we first asked what affinity ranges are relevant. Many known inhibitors have 10–20 μM affinity for this enzyme. To be comprehensive, we considered three thresholds of FTI affinity, each at increasingly greater stringency. In the first instance, we considered all those 1692 FTIs known to have 100 μM or better affinity, reasoning that this would allow for the greatest breadth of predictions. We then narrowed our focus to include only those 1423 FTIs with 10 μM or better affinity and finally excluded all but the 1188 FTIs with affinity $\leq 1 \mu\text{M}$. We considered each threshold independently and later extracted each commercial drug's best SEA match with the set of known PFTase ligands at any of the three thresholds. For example, Loratadine matched most strongly against the FTIs known to have $\leq 10 \mu\text{M}$ for their target, with a SEA expectation value (*E*-value) of 1.07×10^{-81} (Table 1). On the other hand, Ubenimex was most similar to the $\leq 100 \mu\text{M}$ FTIs, with an *E*-value of 1.53×10^{-16} for them (Table 1) compared to weaker *E*-values of 4.97×10^{-13} and 7.23×10^{-9} for its similarity against the $\leq 10 \mu\text{M}$ and $\leq 1 \mu\text{M}$ FTIs, respectively (Table 2). An *E*-value, much like a *p*-value, denotes the likelihood of a particular event. In this case, the *E*-value represents the degree of chemical similarity for a commercial drug against the set of ligands for protein farnesyltransferase as compared to the similarity that would have been found by random chance alone. When applied across all 746 commercial drugs, this analysis found 13 of them (comprising 1.9% of the total drugs screened) to have measurable similarity to at least one of the three FTI sets (Table 1).

Table 2. SEA Predictions for Potential PFTase Ligands at Various Thresholds of Similarity to Known Ligands and Their Subsequent Analysis as PFTase Inhibitors^a

	Drug	SEA similarity to FTIs, by affinity threshold 1 μ M / 10 μ M / 100 μ M	Closest known ligand	IC ₅₀ (μ M)
1	Loratadine 	7.87×10^{-53} 1.07×10^{-81} 1.53×10^{-81}	 0.700 Tc	13.3 ± 1.8
2	Rupatadine 	5.90×10^{-41} 1.10×10^{-49} 8.15×10^{-49}	 0.651 Tc	76 ± 18
3	Desloratadine 	3.45×10^{-27} 1.22×10^{-30} 1.83×10^{-30}	 0.561 Tc	> 100
4	Ubenimex 	7.23×10^{-9} 4.97×10^{-13} 1.53×10^{-16}	 0.453 Tc	> 200
5	Miconazole 	8.26×10^{-2} 2.86×10^{-3} 2.00×10^{-4}	 0.459 Tc	18.9 ± 3.6
6	Econazole 	N/A	 0.452 Tc	23.3 ± 2.0

^aSEA *E*-values are shown denoting the statistical significance of each drug's similarity to known FTIs. The more the *E*-value approaches zero, the more significant the similarity; the strongest prediction for each drug is in bold. Each drug was compared against three different sets of known FTIs. For instance, for the "1 μ M FTIs" set, we only considered those FTIs known to have 1 μ M affinity or greater for PFTase. For the "10 μ M FTIs" set, we considered all FTIs known to have 10 μ M or greater affinity for PFTase, etc. Where a drug's PFTase predictions by SEA are very close (within approximately a single order of magnitude), both *E*-values are bolded.

Several of the predictions have relatively modest SEA values (Table 1). Formally, SEA *E*-values have the same meaning as the more familiar BLAST *E*-values, quantifying the expectation that an observed similarity would occur by chance. The underlying expectation of randomness is, of

course, different for the mostly synthetic annotated ligands analyzed by SEA and naturally evolved sequences, and a pragmatic *E*-value cutoff for making a prediction is not yet clear. In earlier work, we have often looked for *E*-values better (lower) than 10^{-10} , but this is an arbitrary and

conservative cutoff, and novel, potent off-target effects have been predicted based on SEA values as low as 10^{-4} for Vadilex's activity against serotonin transporter, for activity of RO-25-6981 against the κ opioid receptor, 5×10^{-6} for dimethyltryptamine's activity against the 5HT_{5A} receptor and 10^{-7} for Paroxetine's activity against the $\alpha 1$ adrenergic receptor.⁸ Currently, the choice of *E*-value cutoff for testing predictions will vary depending on pragmatic considerations, including the intrepidity of the experimental team. In principle, an *E*-value below 1 is significant.

Of the 12 commercial drugs predicted to have off-target PFTase binding by SEA, 7 already had literature precedent or were difficult to source (see General Materials and Methods). We tested the remaining 5 by in vitro analysis and advanced two to analysis in a mammalian cell line engineered for monitoring the prenylation of H-Ras.³⁹

In Vitro Analysis of PFTase Inhibition. A continuous-fluorescence assay, based on the time-dependent increase in dansyl group fluorescence that occurs as the CAAX-peptide *N*-dansyl-GCVLS is prenylated,^{40,41} was employed to measure PFTase activity in the presence of the predicted inhibitors. This assay was used to calculate IC₅₀ values; for confirmation, the extent of inhibition at the IC₅₀ concentration was confirmed for each compound in a separate HPLC-based assay.⁴² The five commercial drugs tested were comprised of three histamine H₁ receptor antagonists (Loratadine, Desloratadine, and Rupatadine), an antineoplastic (Ubenimex), and an azole antifungal (Miconazole) (Table 1). In our enzymatic assay, two of the antihistamines and the azole antifungal were effective inhibitors of PFTase in the low-to-mid micromolar range (Table 2). For all but Ubenimex, the 100 and 10 μ M FTI sets resulted in the strongest SEA predictions, with little difference in prediction strength between the two affinity classes (Table 2). This was consistent with their calculated PFTase IC₅₀ values, which we found to be between 20 and 80 μ M, with the exception of Desloratadine and Ubenimex, which did not inhibit PFTase up to 100 and 200 μ M, respectively.

After conducting this work, we discovered that analogues of Loratadine have been investigated for PFTase inhibition via a high-throughput screening approach;⁴³ Miconazole, to the best of our knowledge, is a novel PFTase inhibitor class. We thus asked whether other azole antifungals, not predicted by SEA but established members of that class, also had unreported activity with PFTase, controlling for the nonspecific small-molecule aggregation in which some azoles are known to participate.⁴⁴ To this end, we tested the nonaggregators Econazole, Fluconazole, and Ketconazole and the aggregator Clotrimazole in our continuous fluorescence assay.⁴⁵ In accordance with previous work on preventing nonspecific enzyme inhibition by small molecule aggregation,⁴⁵ Triton X-100 was included in all assay solutions to prevent aggregate formation. A nonazole, small molecule aggregator, Tetraiodophenolphthalein (TIPT), previously shown to nonspecifically inhibit enzymes via this mechanism,⁴⁴ was also tested for PFTase inhibition as an internal control. Only Econazole showed appreciable inhibition of PFTase with an IC₅₀ value similar to that measured for Miconazole. The other azole antifungals, including the known aggregator Clotrimazole, showed little to no inhibition at concentrations as high as 100 μ M. TIPT was not an inhibitor of PFTase, confirming that the assay conditions did not allow for in vitro small-molecule aggregation.

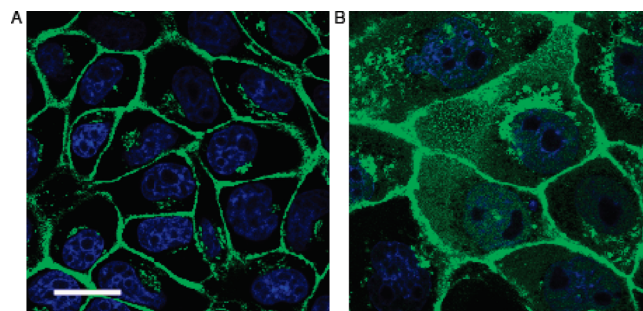


Figure 1. Intracellular inhibition of H-Ras processing by Loratadine (1). Scale bar represents 10 μ m. GFP-H-Ras is shown in green. The cell nucleus is shown in blue. (A) Cells grown in FBS supplemented DMEM containing 0.5% DMSO for 24 h. (B) Cells grown in FBS supplemented DMEM containing 0.5% DMSO and 25 μ M Loratadine for 24 h.

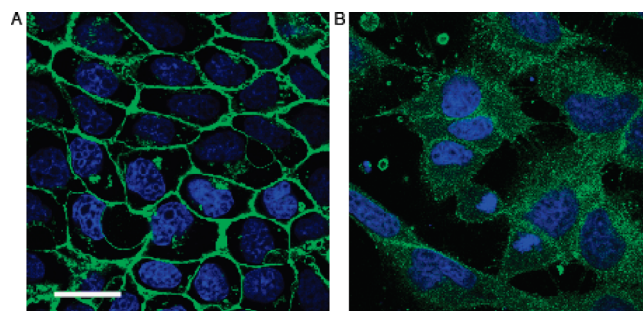


Figure 2. Intracellular inhibition of H-Ras processing by Miconazole (5). Scale bar represents 10 μ m. GFP-H-Ras is shown in green. The cell nucleus is shown in blue. (A) Cells grown in FBS supplemented DMEM containing 0.5% DMSO for 48 h. (B) Cells grown in FBS supplemented DMEM containing 0.5% DMSO and 10 μ M Miconazole for 48 h.

Analysis of Loratadine and Miconazole Using a Cell Based in Vitro Assay. For a FTI to have clinical relevance, it must block the targets of protein farnesylation from functioning properly. A mammalian cell line engineered to express a chimera of the green fluorescent protein (GFP) and H-Ras⁴⁶ was employed to assess the ability of Loratadine and Miconazole to block the membrane localization of Ras through inhibition of farnesylation. GFP-H-Ras that has been processed by PFTase, and the subsequent enzymes in the protein prenylation pathway, will be localized at the cell's Golgi and plasma membrane. If prenylation has been inhibited, GFP-H-Ras will be present in the cellular cytosol.

Cells were treated for 24 h with varying concentrations of Loratadine and Miconazole in DMSO ranging from $1 \times$ to $5 \times$ the experimentally observed enzymatic IC₅₀ value or DMSO vehicle alone. At 25 μ M Loratadine ($2.5 \times$ the IC₅₀) appreciable inhibition of GFP-H-Ras processing was observed as evidenced by the diffuse cytosolic fluorescence not present when treated with DMSO alone (Figure 1). Localization of fluorescence at the Golgi and plasma membrane is also evident, meaning either total inhibition of the GFP-H-Ras was not achieved or GFP-H-Ras synthesized and processed prior to treatment had not been degraded yet. Treating cells with higher concentrations of Loratadine was toxic and led to death, while lower concentrations did not manifest observable inhibition of prenylation. Treatment of cells with Miconazole at concentrations at or above the IC₅₀ value also led to toxicity and cell death. Therefore, treating with 10 μ M Miconazole ($0.5 \times$ the IC₅₀) for 48 h was tested.

A number of cells died in this case and were subsequently washed from the plate during nuclear staining procedure (see General Materials and Methods), but those cells remaining alive and still adhered to the plate had significant inhibition of GFP-H-Ras processing (Figure 2).

Discussion

Whereas the previous drug polypharmacology predicted by SEA focused on drugs that target aminergic GPCRs,^{6–8} Loratadine and Miconazole were predicted to bind PFTase in violation of these traditional target-class boundaries. The antihistamine Loratadine represents one of the first uses of this approach to demonstrate that a commercial drug thought to be specific for a GPCR also binds an enzyme, while the activity of the antifungal P450 Miconazole represents the approach's first enzyme–enzyme cross-talk prediction among commercial drugs. While the IC₅₀ values obtained for these compounds against PFTase are modest at best, they do offer starting points for inhibitor design optimization.

Loratadine is a second-generation antihistamine that binds the H₁ receptor—a cross-membrane target that shares no evolutionary history, functional role, or structural similarity with the enzyme PFTase. We found Loratadine to have an exceptionally strong *E*-value of 1.07×10^{-81} for PFTase ligands in the 10–100 μ M range (Table 2), and SEA also predicted strong scores for two of its analogues, Rupatadine and Desloratadine (1.10×10^{-49} and 1.22×10^{-30} , respectively, Table 2). These off-target predictions were confirmed for Loratadine and Rupatadine, at 13 and 76 μ M IC₅₀s, whereas Desloratadine, the primary metabolite of both Loratadine and Rupatadine, showed no appreciable inhibition up to 100 μ M. For Loratadine, the ability to block the processing of H-Ras in vivo was also confirmed in our GFP-H-Ras chimera mammalian cell line. Loratadine has been reported to be active only at the histamine H₁ receptor,⁴⁷ while Rupatadine is active at both the histamine H₁ and platelet-activating factor receptors.⁴⁸ Both, as well as Desloratadine, have shown good safety profiles over prolonged treatment.^{47,49,50} Antimuscarinic receptor activity, often associated with the earlier generation of H₁ receptor antagonists, is not commonly observed with these drugs.^{51,52}

Whether or not the off-target inhibition of PFTase by Loratadine has any clinical relevance has yet to be determined. At therapeutic doses, the active metabolite of Loratadine (Desloratadine) reaches plasma concentrations of approximately 300 nM (based on information available in DRUGDEX).⁵³ In our study, Desloratadine was not an inhibitor of PFTase. While it appears that Loratadine will not have any clinical significance in terms of PFTase inhibition, synergistic effects with other drugs known to affect protein prenylation levels, such as the commonly prescribed statin drugs that inhibit HMG-CoA reductase,^{54,55} may reveal themselves. An extensive literature search revealed no evidence toward clinical off-label use of Loratadine for the indications related to PFTase. Recently, a high-throughput screening of commercial drugs for toxicity toward the parasite *T. cruzi* revealed Loratadine to have an IC₅₀ value 23 μ M.⁵⁶ Inhibition of *T. cruzi* PFTase could be the cause of this observed toxicity and warrants further investigation. The presence of such off-target drug activity across GPCR and enzyme class boundaries even among well-studied commercial drugs suggests opportunities for both drug development and potential side-effect management. Whether or not

the compounds developed as FTIs have any activity against the histamine H₁ receptor have yet to be investigated or reported.

Miconazole and Econazole are topical imidazole antifungals that increase cell membrane permeability in fungi, resulting in leakage of cellular contents. Both of these antifungals inhibit 14- α demethylase, a cytochrome P-450 enzyme necessary to convert lanosterol to ergosterol, which is an essential component of cell membranes.⁵³ Using SEA, we found that Miconazole had weak yet significant similarity to the set of 100 μ M PFTase inhibitors, with an *E*-value of 2.00×10^{-4} (Table 1). Upon validating Miconazole's 19 μ M IC₅₀ for PFTase, we also tested Econazole, which has a highly similar chemical structure, and found it to have an IC₅₀ of 23 μ M against this target (Table 2). Analyses of Miconazole's ability to block prenylation in vivo revealed it to be toxic at concentrations high enough to result in observable inhibition. The inhibition of ergosterol biosynthesis contributes to Miconazole's antifungal mechanism of action and also, it is thought, to Miconazole's activity against the parasite *T. cruzi*.⁵⁷ It is intriguing to consider that interactions with PFTase may complement the drugs' antifungal and antiparasitic activity. Nonetheless, the enzymes PFTase and 14- α demethylase share no evolutionary history or structural similarity, and this cross talk may suggest new directions for antifungal development.

There is no evidence in the literature pertaining to the use of Miconazole for indications related to PFTase. On the basis of the information available in the DRUGDEX system,⁵³ the peak concentration of Miconazole reached in the body upon subcutaneous delivery (the common dosage form) is approximately 25 nM. This is well below our experimental IC₅₀ value, suggesting that topical administration of Miconazole does not have any clinical significance in terms of PFTase inhibition. It is interesting to note that Miconazole has been tested by the NCI/NIH Developmental Therapeutics Program as an anticancer agent. According to the NCI/DTP Open Chemical Repository (NSC 170986), intraperitoneal delivery of Miconazole was shown to promote survival in mouse models of leukemia and melanoma.⁵⁸ While FTIs are not currently being explored in the treatment of melanoma, they are candidate leukemia chemotherapeutics.^{28,29} Compounds developed as inhibitors of PFTase have not been reported to bind 14- α demethylase.

Conclusions

From a target-based perspective, the activities of Loratadine and Miconazole against PFTase are perplexing—neither the H₁ histamine GPCR nor the fungal P450 have detectable sequence or structural similarity to protein farnesyltransferase. From an older, classical pharmacology perspective, the cross-reactivities are perhaps less surprising, as many drugs share common provenances as chemical series. What recent cheminformatics-based approaches^{5,10–15} bring to this older view is a systematic analysis of all drug space (allowed by the creation of target-ligand annotation databases like WOMBAT⁵⁹ and ChEMBL StARlite⁶⁰) and quantitative models that separate similarity expected at random from similarity that is quantifiably significant among ligand sets. A contribution of this work is to suggest that the similarities observed among targets, based on their ligands, may cross receptor–enzyme and enzyme–enzyme boundaries, and thus techniques that exploit a ligand-based view of pharmacology may have a wide application.⁶⁰

Experimental Section

General Materials and Methods. All tested compounds were purchased from LKT Laboratories (St. Paul, MN) at >98% purity as determined by HPLC. All other reagents were purchased from Sigma Aldrich. *N*-Dansyl-GCVLS was prepared as described in Gaon et al.⁶¹ The PFTase utilized was obtained and purified as described in DeGraw et al.⁶² Fluorescence measurements were made on a Beckman Coulter DTX 880 plate reader fitted with a 340 nm excitation filter and 535 nm emission filter. Hoescht nuclear dye was obtained from Invitrogen.

Sources of Known Protein Farnesyltransferase Ligands. We used several subsets of the known FTIs as our reference sets. To do so, we built the set of known ligands corresponding to each major drug target in the literature extracted from the World of Molecular BioAcTivity (WOMBAT) 2006.2 database, as in previous work.⁶ After removal of duplicates, molecules that we could not process, and ligands with affinities worse than 100 μ M for their protein targets, this database comprised 169046 molecules annotated into 1469 target-function sets (e.g., the PFTase inhibitors and the PFTase binders of unknown function comprised two distinct sets). We then extracted the 1723 molecules from this collection that were annotated as PFTase inhibitors (1648 molecules) or PFTase binders (75 molecules) and filtered out all molecules containing two sequential peptide bonds along a standard peptide backbone, using a SMARTS filter in Scitegic PipelinePilot. We further subdivided these PFTase binders (collectively termed “FTIs” or “FTI sets” in main text) by their affinities for PFTase, into 100, 10, and 1 μ M FTI sets containing 1692, 1423, and 1188 molecules, respectively. The remaining 1467 target-function sets from WOMBAT were not considered in this analysis.

PFTase ligands used in the WOMBAT training sets included few marketed drugs. One exception, cortisone acetate, has an IC_{50} of 14 μ M for PFTase.⁶³ Second, the amino-bisphosphonates ibandronic acid, pamidronic acid, risedronic acid, and alendronic acid, were included in the 1 μ M PFTase ligand set due to their annotations in WOMBAT, although subsequent investigation revealed that direct binding of these bisphosphonates to PFTase has not been demonstrated, to our knowledge. The remaining marketed drugs shown in Table 1 were not included in the training sets, as they were not reported as PFTase ligands in WOMBAT.

Choice of Ligand Set Thresholds. While we included a PFTase ligand set at 100 μ M for completeness and to increase the chance of finding novel PFTase ligands, we note that SEA predictions for ligand sets at 10 μ M compared to those at 100 μ M did not substantially differ. Ubenimex was the only exception (Table 2), and in this case, the SEA prediction yielded no detectable binding at <100 μ M. Ligand set thresholds of 1 and 10 μ M may be sufficient for future analysis directed at PFTase.

Collection of Commercial Drugs. We extracted all molecules annotated as marketed drugs in the WOMBAT 2006.2 database and processed them as above (excepting peptide and 100 μ M affinity filtering). This yielded 746 commercial drugs, each of which we screened individually against the FTI sets using SEA.

Similarity Measures. We used 1024-bit folded Scitegic ECFP_4 topological fingerprints as previously described.⁶ Although we later also tested 2048-bit Daylight^{6,7} fingerprints, these resulted in a narrower and weaker subset of the PFTase predictions found via ECFP_4 and are not reported here. As before, we used the Tanimoto coefficient to calculate pairwise similarity between fingerprints.^{6,7}

Similarity Ensemble Approach (SEA). SEA is based on the premise that chemically similar molecules will bind similar targets^{64,65} and thus have similar biological profiles.⁶⁶ A raw score is calculated for ligand set similarity by summing the Tanimoto similarities^{67–69} between all ligand sets of interest. This score in itself is not an accurate assessment of similarity because it is dependent on the number of ligands in each set and

it does not take into account random similarities. Set-size dependence is corrected for by SEA using a statistically determined threshold. Pairs of molecules that score below it are discarded and do not contribute to the overall set similarity. The raw score gets converted to a *z*-score, free of set-size bias, using the mean and standard deviation of raw scores modeled from sets of random molecules. The final similarity score is expressed as an expectation value (*E*-value) based on the probability of observing a given *z*-score using random data. Small *E*-values reflect relationships between ligand sets that are stronger than would be expected by random chance alone. SEA effectively links ligand sets and their corresponding protein targets together in minimal spanning trees, resulting in biological related proteins being clustered together.

Predictions of Off-Target PFTase Binding Using SEA. We ran SEA as previously described.⁷ The query collection consisted of the 746 commercial drugs, each drug as its own “set” of one molecule. The reference collection comprised the three overlapping sets of PFTase ligands (“FTIs”), binned into each set at (a) 1 μ M, (b) 10 μ M, or (c) 100 μ M affinity thresholds. A FTI set with a weaker affinity threshold, such as 100 μ M, comprised an all-inclusive superset of those sets at stronger affinity threshold (both the 1 and 10 μ M sets, in this example). After each drug was compared independently against each of the three FTI sets by SEA, their *E*-values were compared (e.g., see Table 2) and all commercial drugs with measurable best-match *E*-values across sets were reported (Table 1).

Choice of Drugs for Testing. We excluded Diazepam and Temazepam because Diazepam’s weak PFTase activity is already reported⁷⁰ and the steroids because Cortisone’s and Prednisone’s PFTase activities are likewise known.⁶³ We chose not to pursue Azatadine due to sourcing issues and did not test Thymopentin or Phenylalanine-S because they are peptides. We excluded both the known peptide FTIs and the predicted peptide drugs because SEA’s statistical models were built using small-molecule drug chemical similarity descriptors. As peptides contain oft-repeated chemical patterns in their backbones, and thus strong opportunities for *uninformative* similarity, they may have the potential to skew small-molecule similarity models if included. We nonetheless tested one peptide prediction, Ubenimex, because it appeared highly similar to a known FTI.

PFTase in Vitro Assay. The continuous fluorescence assay developed by Pompliano and co-workers⁴¹ was adapted to a 96-well plate format. Assay solutions in individual wells contained 50 mM Tris-HCl, pH 7.5, 10 mM MgCl₂, 10 μ M ZnCl₂, 5.0 mM DTT, 0.02% (w/v) *n*-octylglucopyranoside, 2.0 μ M *N*-dansyl-GCVLS, FPP (10 μ M), and inhibitor at varying concentrations (from 0 to 200 μ M). All inhibitors were dissolved in DMSO due to limited solubility. For analysis of the H1 receptor agonists, a total of 5% (v/v) DMSO was in each sample. For analysis of the azole antifungals, a total of 20% (v/v) DMSO was in each sample as well as 0.04% (v/v) Triton X-100 to prevent aggregate formation. Each sample was analyzed in triplicate. PFTase was prepared by diluting purified enzyme with buffer (52 mM Tris-HCl, pH 7.0, 5.8 mM DTT, 12 mM MgCl₂, 12 μ M ZnCl₂) containing 1 mg/mL bovine serum albumin. Samples were equilibrated at 30 °C, and the reaction was initiated by the addition of dilute PFTase. Fluorescence intensity was monitored via a time-based scan for 60 min or longer depending on when fluorescence enhancement ceased. The enzymatic rate of each reaction was determined by converting the rate of increase in fluorescence intensity units (FIU/s) to μ M/s with eq 1,

$$v_i = \frac{RP}{F_{\max}} \quad (1)$$

where v_i is the enzymatic rate in μ M/s, R is the measured rate in FIU/s, and P is the concentration of *N*-dansyl-GCVLS used in the assay. F_{\max} is the fluorescence intensity of the fully prenylated peptide.

Cell Based Analysis of H-Ras Processing. MDCK cells engineered to overexpress a GFP-H-Ras chimera were used to visualize Ras processing in vivo. For all experiments, 2.6×10^4 cells/cm² were seeded in culture dishes. The cells were grown in DMEM media supplemented with 10% fetal bovine serum at 37 °C with 5.0% CO₂ and grown to approximately 50% confluency (generally 24 h). The cells were then washed twice with serum-free DMEM and fresh serum-free DMEM was added. The desired inhibitor (Loratadine or Miconazole) in DMSO was added at varying concentrations (1–200 μ M drug, 0.5–1.0% (v/v) DMSO) and incubated for 24 h at 37 °C and 5.0% CO₂. Hoechst 34580 nuclear stain was added to a final concentration of 1 μ g/mL during the final 20 min of incubation. The cells were then washed twice with PBS and placed back in DMEM. Imaging was performed on an Olympus FluoView 1000 confocal microscope with a 60 \times objective. The Hoechst 34580 nuclear stain was imaged with 405 nm excitation and 461 nm emission. The GFP-H-Ras chimera was imaged with 488 nm excitation and 519 nm emission.

Acknowledgment. This work is supported by the National Institutes of Health grants GM58442 (M.D.D.) and GM71896 (B.K.S.), a National Institutes of Health Training grant T32-GM000347 (A.J.D.), and a National Science Foundation fellowship (M.J.K.). We thank Sunset Molecular Discovery LLC for the use of WOMBAT. We thank Nicholette Zeliadt and Professor Elizabeth Wattenberg (University of Minnesota) for providing the MDCK cells, space to perform cell cultures, and technical assistance. The MDCK cells were a generous gift from Professor Mark Philips, New York University School of Medicine. We thank J. C. Engel and the Sandler Center for Basic Research in Parasitic Diseases for access to unpublished Loratadine IC₅₀ results in *T. cruzi*.

References

- Adams, C. P.; Brantner, V. V. Estimating the cost of new drug development: is it really 802 million dollars? *Health Aff. (Millwood)* **2006**, *25*, 420–428.
- Hopkins, A. L. Network pharmacology: the next paradigm in drug discovery. *Nat. Chem. Biol.* **2008**, *4*, 682–690.
- Oprea, T. I.; Tropsha, A.; Faulon, J. L.; Rintoul, M. D. Systems chemical biology. *Nat. Chem. Biol.* **2007**, *3*, 447–450.
- Scheiber, J.; Jenkins, J. L. Chemogenomic analysis of safety profiling data. *Methods Mol. Biol.* **2009**, *575*, 207–223.
- Wermuth, C. G. Selective optimization of side activities: the SOSA approach. *Drug Discovery Today* **2006**, *11*, 160–164.
- Hert, J.; Keiser, M. J.; Irwin, J. J.; Oprea, T. I.; Shoichet, B. K. Quantifying the relationships among drug classes. *J. Chem. Inf. Model.* **2008**, *48*, 755–765.
- Keiser, M. J.; Roth, B. L.; Armbruster, B. N.; Ernsberger, P.; Irwin, J. J.; Shoichet, B. K. Relating protein pharmacology by ligand chemistry. *Nat. Biotechnol.* **2007**, *25*, 197–206.
- Keiser, M. J.; Vincent, S.; Irwin, J. J.; Laggner, C.; Abbas, A. I.; Hufeisen, S. J.; Jensen, N. H.; Kuijer, M. B.; Matos, R. C.; Tran, T. B.; Whaley, R.; Glennon, R. A.; Hert, J.; Thomas, K. L. H.; Edwards, D. D.; Shoichet, B. K.; Roth, B. L. Predicting new molecular targets for known drugs. *Nature* **2009**, *462*, 175–181.
- Bajorath, J. Computational analysis of ligand relationships within target families. *Curr. Opin. Chem. Biol.* **2008**, *12*, 352–358.
- Campillos, M.; Kuhn, M.; Gavin, A. C.; Jensen, L. J.; Bork, P. Drug target identification using side-effect similarity. *Science* **2008**, *321*, 263–266.
- Lounkine, E.; Stumpfe, D.; Bajorath, J. Molecular Formal Concept Analysis for compound selectivity profiling in biologically annotated databases. *J. Chem. Inf. Model.* **2009**, *49*, 1359–1368.
- Muchmore, S. W.; Debe, D. A.; Metz, J. T.; Brown, S. P.; Martin, Y. C.; Hajduk, P. J. Application of belief theory to similarity data fusion for use in analog searching and lead hopping. *J. Chem. Inf. Model.* **2008**, *48*, 941–948.
- Scheiber, J.; Jenkins, J. L.; Sukuru, S. C.; Bender, A.; Mikhailov, D.; Milik, M.; Azzaoui, K.; Whitebread, S.; Hamon, J.; Urban, L.; Glick, M.; Davies, J. W. Mapping adverse drug reactions in chemical space. *J. Med. Chem.* **2009**, *52*, 3103–3107.
- Vieth, M.; Erickson, J.; Wang, J.; Webster, Y.; Mader, M.; Higgs, R.; Watson, I. Kinase inhibitor data modeling and de novo inhibitor design with fragment approaches. *J. Med. Chem.* **2009**, *52*, 6456–6666.
- Young, D. W.; Bender, A.; Hoyt, J.; McWhinnie, E.; Chirn, G. W.; Tao, C. Y.; Tallarico, J. A.; Labow, M.; Jenkins, J. L.; Mitchison, T. J.; Feng, Y. Integrating high-content screening and ligand-target prediction to identify mechanism of action. *Nat. Chem. Biol.* **2008**, *4*, 59–68.
- Altschul, S. F.; Gish, W.; Miller, W.; Myers, E. W.; Lipman, D. J. Basic local alignment search tool. *J. Mol. Biol.* **1990**, *215*, 403–410.
- Keiser, M. J.; Hert, J. Off-target networks derived from ligand set similarity. *Methods Mol. Biol.* **2009**, *575*, 195–205.
- Walsh, C. T.; Garneau-Tsodikova, S.; Gatto, G. J., Jr. Protein posttranslational modifications: the chemistry of proteome diversifications. *Angew. Chem., Int. Ed.* **2005**, *44*, 7342–7372.
- Reid, T. S.; Terry, K. L.; Casey, P. J.; Beese, L. S. Crystallographic Analysis of CaaX Prenyltransferases Complexed with Substrates Defines Rules of Protein Substrate Selectivity. *J. Mol. Biol.* **2004**, *343*, 417–433.
- Zhang, F. L.; Casey, P. J. Protein prenylation: molecular mechanisms and functional consequences. *Annu. Rev. Biochem.* **1996**, *65*, 241–269.
- Lowy, D. R.; Willumsen, B. M. Function and regulation of ras. *Annu. Rev. Biochem.* **1993**, *62*, 851–891.
- Kato, K.; Cox, A. D.; Hisaka, M. M.; Graham, S. M.; Buss, J. E.; Der, C. J. Isoprenoid addition to Ras protein is the critical modification for its membrane association and transforming activity. *Proc. Natl. Acad. Sci. U.S.A.* **1992**, *89*, 6403–6407.
- Bell, I. M. Inhibitors of Farnesyltransferase: A Rational Approach to Cancer Chemotherapy? *J. Med. Chem.* **2004**, *47*, 1869–1878.
- Zhu, K.; Hamilton, A. D.; Sebt, S. M. Farnesyltransferase inhibitors as anticancer agents: current status. *Curr. Opin. Invest. Drugs* **2003**, *4*, 1428–1435.
- Brunner, T. B.; Hahn, S. M.; Gupta, A. K.; Muschel, R. J.; McKenna, W. G.; Bernhard, E. J. Farnesyltransferase inhibitors: an overview of the results of preclinical and clinical investigations. *Cancer Res.* **2003**, *63*, 5656–5668.
- Doll, R. J.; Kirschmeier, P.; Bishop, W. R. Farnesyltransferase inhibitors as anticancer agents: critical crossroads. *Curr. Opin. Drug. Discovery Dev.* **2004**, *7*, 478–486.
- Sparano, J. A.; Moulder, S.; Kazi, A.; Coppola, D.; Negassa, A.; Vahdat, L.; Li, T.; Pellegrino, C.; Fineberg, S.; Munster, P.; Malafa, M.; Lee, D.; Hoschander, S.; Hopkins, U.; Hershman, D.; Wright, J. J.; Kleer, C.; Merajver, S.; Sebt, S. M. Phase II trial of tipifarnib plus neoadjuvant doxorubicin-cyclophosphamide in patients with clinical stage IIB-IIIC breast cancer. *Clin. Cancer. Res.* **2009**, *15*, 2942–2948.
- Karp, J. E.; Flatten, K.; Feldman, E. J.; Greer, J. M.; Loegering, D. A.; Ricklis, R. M.; Morris, L. E.; Ritchie, E.; Smith, B. D.; Ironside, V.; Talbot, T.; Roboz, G.; Le, S. B.; Meng, X. W.; Schneider, P. A.; Dai, N. T.; Adjei, A. A.; Gore, S. D.; Levis, M. J.; Wright, J. J.; Garrett-Mayer, E.; Kaufmann, S. H. Active oral regimen for elderly adults with newly diagnosed acute myelogenous leukemia: a preclinical and phase I trial of the farnesyltransferase inhibitor tipifarnib (R115777, Zarnestra) combined with etoposide. *Blood* **2009**, *113*, 4841–4852.
- Feldman, A. L.; Law, M.; Remstein, E. D.; Macon, W. R.; Erickson, L. A.; Grogg, K. L.; Kurtin, P. J.; Dogan, A. Recurrent translocations involving the IRF4 oncogene locus in peripheral T-cell lymphomas. *Leukemia* **2009**, *23*, 574–580.
- Meta, M.; Yang, S. H.; Bergo, M. O.; Fong, L. G.; Young, S. G. Protein farnesyltransferase inhibitors and progeria. *Trends. Mol. Med.* **2006**, *12*, 480–487.
- Yang, S. H.; Meta, M.; Qiao, X.; Frost, D.; Bauch, J.; Coffinier, C.; Majumdar, S.; Bergo, M. O.; Young, S. G.; Fong, L. G. A farnesyltransferase inhibitor improves disease phenotypes in mice with a Hutchinson–Gilford progeria syndrome mutation. *J. Clin. Invest.* **2006**, *116*, 2115–2121.
- Fong, L. G.; Frost, D.; Meta, M.; Qiao, X.; Yang, S. H.; Coffinier, C.; Young, S. G. A protein farnesyltransferase inhibitor ameliorates disease in a mouse model of progeria. *Science* **2006**, *311*, 1621–1623.
- Gordon, L. B.; Harling-Berg, C. J.; Rothman, F. G. Highlights of the 2007 Progeria Research Foundation scientific workshop: progress in translational science. *J. Gerontol., Ser. A* **2008**, *63*, 777–787.
- Eastman, R. T.; Buckner, F. S.; Yokoyama, K.; Gelb, M. H.; Van Voorhis, W. C. Thematic review series: lipid posttranslational modifications. Fighting parasitic disease by blocking protein farnesylation. *J. Lipid Res.* **2006**, *47*, 233–240.
- Kraus, J. M.; Verlinde, C. L.; Karimi, M.; Lepesheva, G. I.; Gelb, M. H.; Buckner, F. S. Rational modification of a candidate cancer

- drug for use against Chagas disease. *J. Med. Chem.* **2009**, *52*, 1639–1647.
- (36) Ohkanda, J.; Buckner, F. S.; Lockman, J. W.; Yokoyama, K.; Carrico, D.; Eastman, R.; de Luca-Fradley, K.; Davies, W.; Croft, S. L.; Van Voorhis, W. C.; Gelb, M. H.; Sebti, S. M.; Hamilton, A. D. Design and synthesis of peptidomimetic protein farnesyltransferase inhibitors as anti-*Trypanosoma brucei* agents. *J. Med. Chem.* **2004**, *47*, 432–445.
- (37) Carrico, D.; Ohkanda, J.; Kendrick, H.; Yokoyama, K.; Blaskovich, M. A.; Bucher, C. J.; Buckner, F. S.; Van Voorhis, W. C.; Chakrabarti, D.; Croft, S. L.; Gelb, M. H.; Sebti, S. M.; Hamilton, A. D. In vitro and in vivo antimalarial activity of peptidomimetic protein farnesyltransferase inhibitors with improved membrane permeability. *Bioorg. Med. Chem.* **2004**, *12*, 6517–6526.
- (38) Ohkanda, J.; Lockman, J. W.; Yokoyama, K.; Gelb, M. H.; Croft, S. L.; Kendrick, H.; Harrell, M. I.; Feagin, J. E.; Blaskovich, M. A.; Sebti, S. M.; Hamilton, A. D. Peptidomimetic inhibitors of protein farnesyltransferase show potent antimalarial activity. *Bioorg. Med. Chem. Lett.* **2001**, *11*, 761–764.
- (39) Keller, P. J.; Fiordalisi, J. J.; Berzat, A. C.; Cox, A. D. Visual monitoring of post-translational lipid modifications using EGFP-GTPase probes in live cells. *Methods* **2005**, *37*, 131–137.
- (40) Cassidy, P. B.; Dolence, J. M.; Poulter, C. D. Continuous fluorescence assay for protein prenyltransferases. *Methods Enzymol.* **1995**, *250*, 30–43.
- (41) Pompliano, D. L.; Gomez, R. P.; Anthony, N. J. Intramolecular fluorescence enhancement: a continuous assay of Ras farnesyl: protein transferase. *J. Am. Chem. Soc.* **1992**, *114*, 7945–7946.
- (42) Wollack, J. S., Jr.; Petzold, C.; Mougous, J.; Distefano, M. D. A Minimalist Substrate for Enzymatic Peptide and Protein Conjugation. *ChemBioChem* **2009**, *10*, 2934–2943.
- (43) Njoroge, F. G.; Doll, R. J.; Vibulbhan, B.; Alvarez, C. S.; Bishop, W. R.; Petrin, J.; Kirschmeier, P.; Carruthers, N. I.; Wong, J. K.; Albanese, M. M.; Piwinski, J. J.; Catino, J.; Girijavallabhan, V.; Ganguly, A. K. Discovery of novel nonpeptide tricyclic inhibitors of Ras farnesyl protein transferase. *Bioorg. Med. Chem.* **1997**, *5*, 101–113.
- (44) Coan, K. E.; Shoichet, B. K. Stoichiometry and physical chemistry of promiscuous aggregate-based inhibitors. *J. Am. Chem. Soc.* **2008**, *130*, 9606–9612.
- (45) Feng, B. Y.; Simeonov, A.; Jadhav, A.; Babaoğlu, K.; Inglese, J.; Shoichet, B. K.; Austin, C. P. A high-throughput screen for aggregation-based inhibition in a large compound library. *J. Med. Chem.* **2007**, *50*, 2385–2390.
- (46) Choy, E.; Chiu, V. K.; Silletti, J.; Feoktistov, M.; Morimoto, T.; Michaelson, D.; Ivanov, I. E.; Philips, M. R. Endomembrane trafficking of ras: the CAAX motif targets proteins to the ER and Golgi. *Cell* **1999**, *98*, 69–80.
- (47) Morgan, M. M.; Khan, D. A.; Nathan, R. A. Treatment for allergic rhinitis and chronic idiopathic urticaria: focus on oral antihistamines. *Ann. Pharmacother.* **2005**, *39*, 2056–2064.
- (48) Picado, C. Rupatadine: pharmacological profile and its use in the treatment of allergic disorders. *Expert Opin. Pharmacother.* **2006**, *7*, 1989–2001.
- (49) Bachert, C. A review of the efficacy of desloratadine, fexofenadine, and levocetirizine in the treatment of nasal congestion in patients with allergic rhinitis. *Clin. Ther.* **2009**, *31*, 921–944.
- (50) Mullol, J.; Bousquet, J.; Bachert, C.; Canonica, W. G.; Gimenez-Arnau, A.; Kowalski, M. L.; Marti-Guadano, E.; Maurer, M.; Picado, C.; Scadding, G.; Van Cauwenberge, P. Rupatadine in allergic rhinitis and chronic urticaria. *Allergy* **2008**, *63*, 5–28.
- (51) Liu, H.; Farley, J. M. Effects of first and second generation antihistamines on muscarinic induced mucus gland cell ion transport. *BMC Pharmacol.* **2005**, *5*, 8.
- (52) Howell, G., III; West, L.; Jenkins, C.; Lineberry, B.; Yokum, D.; Rockhold, R. In vivo antimuscarinic actions of the third generation antihistaminergic agent, desloratadine. *BMC Pharmacol.* **2005**, *5*, 13.
- (53) *DRUGDEX MICROMEDEX*; Thomson Reuters: Greenwood Village, CO, 2008.
- (54) Ogunwobi, O. O.; Beales, I. L. Statins inhibit proliferation and induce apoptosis in Barrett's esophageal adenocarcinoma cells. *Am. J. Gastroenterol.* **2008**, *103*, 825–837.
- (55) Farwell, W. R.; Scranton, R. E.; Lawler, E. V.; Lew, R. A.; Brophy, M. T.; Fiore, L. D.; Gaziano, J. M. The association between statins and cancer incidence in a veterans population. *J. Natl. Cancer Inst.* **2008**, *100* (2), 134–139.
- (56) Engel, J. C. **2009**, unpublished.
- (57) Docampo, R.; Moreno, S. N. J.; Turrens, J. F.; Katzin, A. M.; Gonzalez-Cappa, S. M.; Stoppani, A. O. M. Biochemical and ultrastructural alterations produced by miconazole and econazole in *Trypanosoma cruzi*. *Mol. Biochem. Parasitol.* **1981**, *3*, 169–180.
- (58) National Cancer Institute. *The NCI/DTP Open Chemical Repository*; NSC agent numbers 170986 and 169434, **2009**; <http://dtp.cancer.gov>.
- (59) Olah, M.; Rad, R.; Ostopovici, L.; Bora, A.; Hadaruga, N.; Hadaruga, D.; Moldovan, R.; Fulias, A.; Mracec, M.; Oprea, T. I.; WOMBAT and WOMBAT-PK: Bioactivity Databases for Lead and Drug Discovery. In *Chemical Biology: From Small Molecules to Systems Biology and Drug Design*; Schreiber, S. L., Kapoor, T. M., Wess, G., Ed.; Wiley-VCH: New York, 2007; pp 760–786.
- (60) *EMBL-EBI, ChEMBL, StARlite*, **2009**; <http://www.ebi.ac.uk/chembl/>.
- (61) Gaon, I.; Turek, T. C.; Weller, V. A.; Edelstein, R. L.; Singh, S. K.; Distefano, M. D. Photoactive Analogs of Farnesyl Pyrophosphate Containing Benzoylbenzoate Esters: Synthesis and Application to Photoaffinity Labeling of Yeast Protein Farnesyltransferase. *J. Org. Chem.* **1996**, *61*, 7738–7745.
- (62) DeGraw, A. J.; Hast, M. A.; Xu, J.; Mullen, D.; Beese, L. S.; Barany, G.; Distefano, M. D. Caged protein prenyltransferase substrates: tools for understanding protein prenylation. *Chem. Biol. Drug Des.* **2008**, *72*, 171–181.
- (63) Lingham, R. B.; Silverman, K. C.; Jayasuriya, H.; Kim, B. M.; Amo, S. E.; Wilson, F. R.; Rew, D. J.; Schaber, M. D.; Bergstrom, J. D.; Koblan, K. S.; Graham, S. L.; Kohl, N. E.; Gibbs, J. B.; Singh, S. B. Clavarinic acid and steroidal analogues as Ras- and FPP-directed inhibitors of human farnesyl-protein transferase. *J. Med. Chem.* **1998**, *41*, 4492–4501.
- (64) Frye, S. V. Structure–activity relationship homology (SARAH); a conceptual framework for drug discovery in the genomic era. *Chem. Biol.* **1999**, *6*, R3–R7.
- (65) Jacoby, E.; Schuffenhauer, A.; Floersheim, P. Chemogenomics knowledge-based strategies in drug discovery. *Drug News Perspect.* **2003**, *16*, 93–102.
- (66) Maggiora, G. M.; Johnson, M. A. Introduction to similarity in chemistry. *Concepts Appl. Mol. Simul.* **1990**, 1–13.
- (67) Altschul, S. F.; Gish, W.; Miller, W.; Myers, E. W.; Lipman, D. J. Basic local alignment search tool. *J. Mol. Biol.* **1990**, *215*, 403–410.
- (68) Karlin, S.; Altschul, S. F. Methods for assessing the statistical significance of molecular sequence features by using general scoring schemes. *Proc. Natl. Acad. Sci. U.S.A.* **1990**, *87*, 2264–2268.
- (69) Pearson, W. R. Empirical statistical estimates for sequence similarity searches. *J. Mol. Biol.* **1998**, *276*, 71–84.
- (70) Roskoski, R., Jr.; Ritchie, P. A. Time-dependent inhibition of protein farnesyltransferase by a benzodiazepine peptide mimetic. *Biochemistry* **2001**, *40*, 9329–9335.